

The background features stylized silhouettes of a satellite in the top left and a telescope in the bottom right, both in shades of grey. The satellite has a central body with several rectangular panels extending outwards. The telescope has a large primary mirror and a secondary mirror mounted on a truss structure.

Constraints on dark matter

from gamma-ray observations

Céline **Armand**



- **Presentation** of the sources and the experiments
- **Data** analysis
- **Statistical** analysis & **Combination**
- **Constraints** on dark matter
- **Conclusions** and perspectives

INDIRECT SEARCHES

Expected γ -ray flux from DM annihilation

Astrophysical
J factor

$$\frac{d\Phi(\langle\sigma v\rangle, J)}{dE} = \frac{1}{4\pi} \frac{\langle\sigma v\rangle}{2m_\chi^2} \sum_f \text{BR}_f \frac{dN_f}{dE} \times \int_{\Delta\Omega} \int_{\text{los}} \rho_{\text{DM}}^2 ds d\Omega$$

Particle Physics
factor

where

$\langle\sigma v\rangle$ = annihilation cross-section

m_χ = DM particle mass

BR_f = branching ratio

dN_f/dE = differential spectrum

ρ_{DM} = DM density

DWARF SPHEROIDAL GALAXIES (dSphs)

A few properties ...

- Located between **~20 kpc and 200 kpc**
- **No rotation**
- **Little or no gas**
- **Old** stellar population
- Dark matter **dominated**



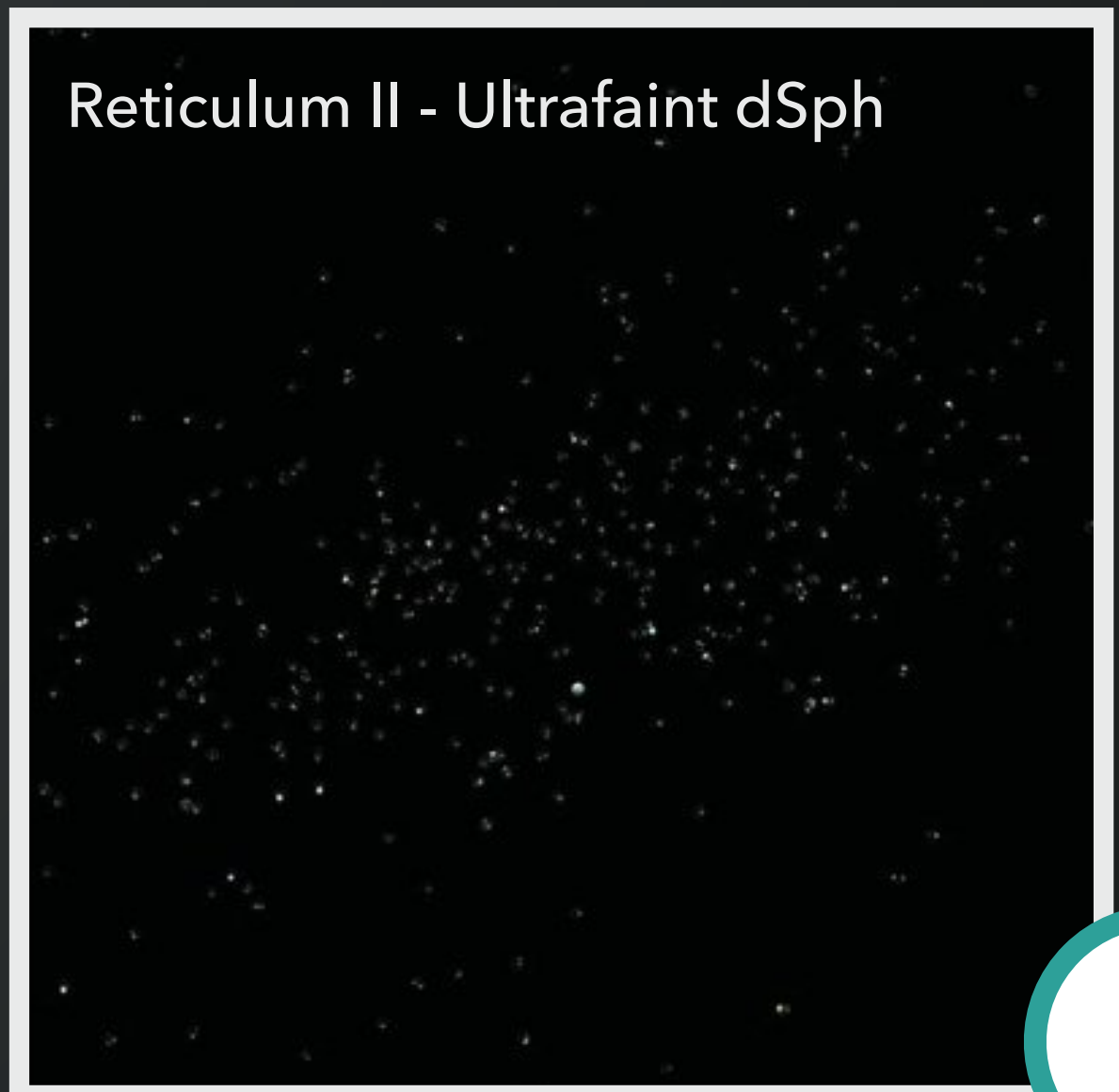
Classicals

~150 - 2500 bright stars
(tracers)



Ultrafaints

- **Higher** J factor
- **~ tens** of bright stars
- **Large uncertainties** on their dark matter distribution



FIVE EXPERIMENTS

All complementary
Cover a wide energy range



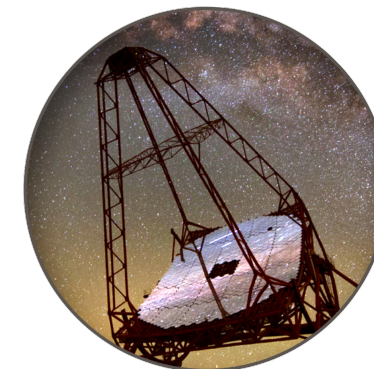
Fermi-LAT
Space telescope
20 MeV to 1 TeV



HAWC
300 water Cherenkov detectors
300 GeV to 100 TeV



VERITAS
4 imaging air Cherenkov telescopes (IACT)
85 GeV to 30 TeV



H.E.S.S.
5 imaging air Cherenkov telescopes (IACT)
30 GeV to 100 TeV



MAGIC
2 imaging air Cherenkov telescopes (IACT)
30 GeV to 100 TeV

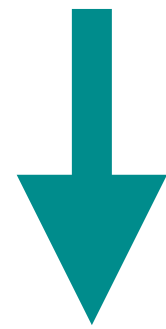
MeV

GeV

TeV

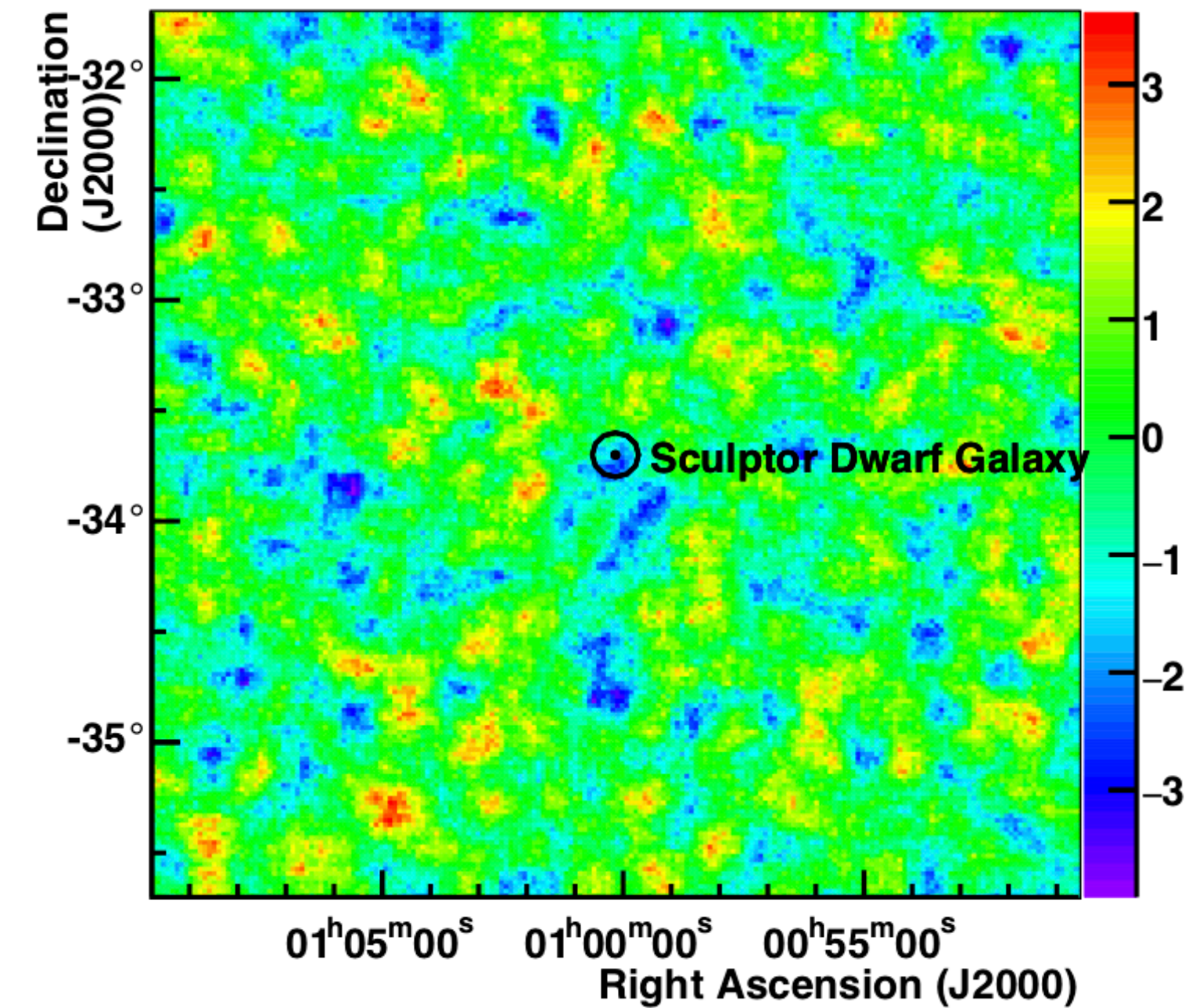
DATA ANALYSIS IN H.E.S.S.

Determination of the **event distributions in energy** of the signal and background regions



Derivation of the **excess and its significance**

Significance Map



No significant excess observed

Data analysis **provides the event distributions and the parameters required** to perform the statistical analysis

STATISTICAL ANALYSIS

LIKELIHOOD FUNCTION

$$\mathcal{L}(\langle \sigma \nu; \nu | \mathcal{D}_{\text{dSphs}}) = \prod_{k=1}^{\text{dSph}} \prod_{l=1}^{\text{Experiment}} \mathcal{L}_{\text{dSph},l,k}(\langle \sigma \nu; J_{l,k}, \nu_{l,k} | \mathcal{D}_{\text{dSphs}}) \mathcal{I}_k(J_k | \bar{J}, \sigma_{\log_{10} J})$$

Likelihood of individual instruments and individual dSphs
J factor nuisance

Product of likelihoods of all energy bins

$$\mathcal{L}_{\text{dSph},l,k} = \prod_{e=1} \mathcal{L}_{P_e}(\langle \sigma \nu \rangle, J | \mathcal{D}_{\text{data}_e})$$

Log-normal likelihood to model the uncertainties of the J factor

$$\mathcal{L}^J = \frac{1}{\ln(10)\sqrt{2\pi}\sigma_J} \exp\left(-\frac{(\log_{10} J - \log_{10} \bar{J})^2}{2\sigma_J^2}\right)$$

STATISTICAL ANALYSIS

LOG-LIKELIHOOD RATIO TEST STATISTICS

Constrained
minimization

$$TS = -2 \ln \frac{\mathcal{L} \left(\langle \sigma \nu \rangle; \hat{\nu} \mid \mathcal{D}_{\text{dSphs}} \right)}{\mathcal{L} \left(\widehat{\langle \sigma \nu \rangle}; \hat{\nu} \mid \mathcal{D}_{\text{dSphs}} \right)}$$

Global
minimization

Ref: Cowan et al. (2011), European
Physical Journal C, vol. 71 p1554

$\langle \sigma \nu \rangle$

Parameter of interest

$\mathcal{D}_{\text{dSph}}$

Data of the dSphs

ν

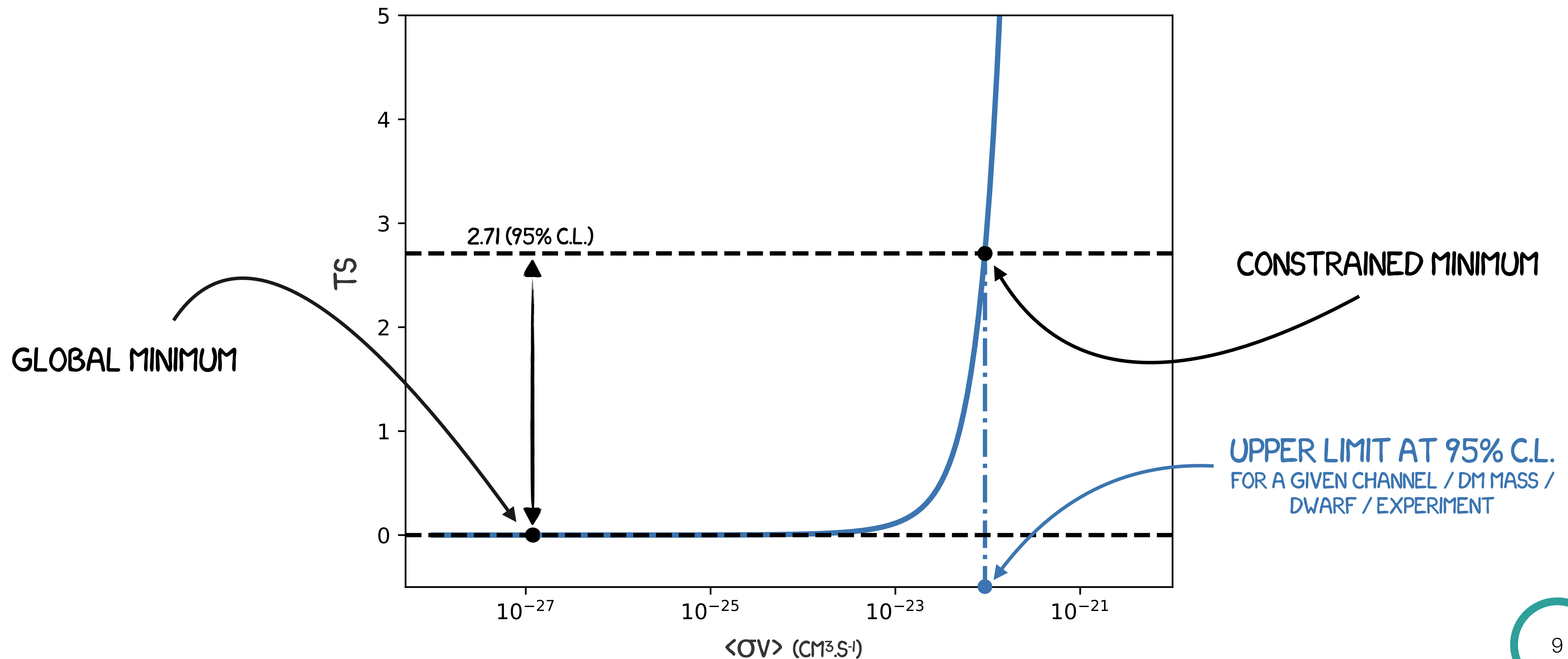
Nuisance parameters

TS

2.71 for 1-sided 95% Confidence Level
and 1 degree of freedom

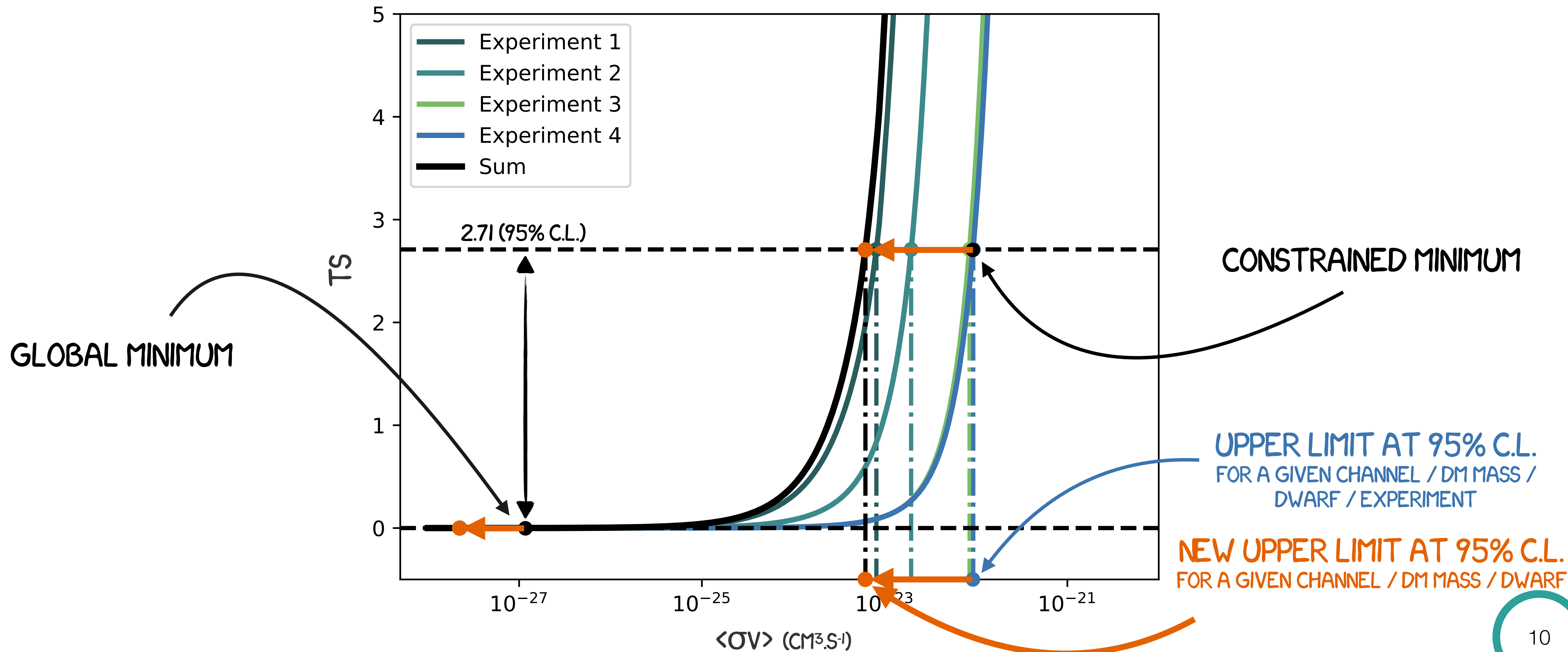
STATISTICAL ANALYSIS

LOG-LIKELIHOOD RATIO TEST STATISTICS



STATISTICAL ANALYSIS

LOG-LIKELIHOOD RATIO TEST STATISTICS



Combined DM search

Source name	Fermi-LAT	HAWC	H.E.S.S, MAGIC, VERITAS		
	Exposure (10^{11} s m ²)	$ \Delta\theta $ (°)	IACT	Zenith (°)	Exposure (h)
Boötes I	2.6	4.5	VERITAS	15 – 30	14.0
Canes Venatici I	2.9	14.6	–	–	–
Canes Venatici II	2.9	15.3	–	–	–
Carina	3.1	–	H.E.S.S.	27 – 46	23.7
Coma Berenices	2.7	4.9	H.E.S.S.	47 – 49	11.4
			MAGIC	5 – 37	49.5
Draco	3.8	38.1	MAGIC	29 – 45	52.1
			VERITAS	25 – 40	49.8
Fornax	2.7	–	H.E.S.S.	11 – 25	6.8
Hercules	2.8	6.3	–	–	–
Leo I	2.4	6.7	–	–	–
Leo II	2.6	3.1	–	–	–
Leo IV	2.4	19.5	–	–	–
Leo V	2.4	–	–	–	–
Leo T	2.6	–	–	–	–
Sculptor	2.7	–	H.E.S.S.	10 – 46	11.8
			MAGIC	13 – 37	158.0
Segue I	2.5	2.9	VERITAS	15 – 35	92.0
			–	–	–
Segue II	2.7	–	–	–	–
Sextans	2.4	20.6	–	–	–
Ursa Major I	3.4	32.9	–	–	–
Ursa Major II	4.0	44.1	MAGIC	35 – 45	94.8
Ursa Minor	4.1	–	VERITAS	35 – 45	60.4

20 dSphs

5 Experiments

16 People

- Observed by one or several experiments
- All previously published by individual collaborations

CONSTRAINTS ON DARK MATTER

- 1 **Observed** limits - Collected data
- 2 **Expected** limits - Sample of **300 Poisson realizations** of the background events produced by individual experiments



Mean expected limits

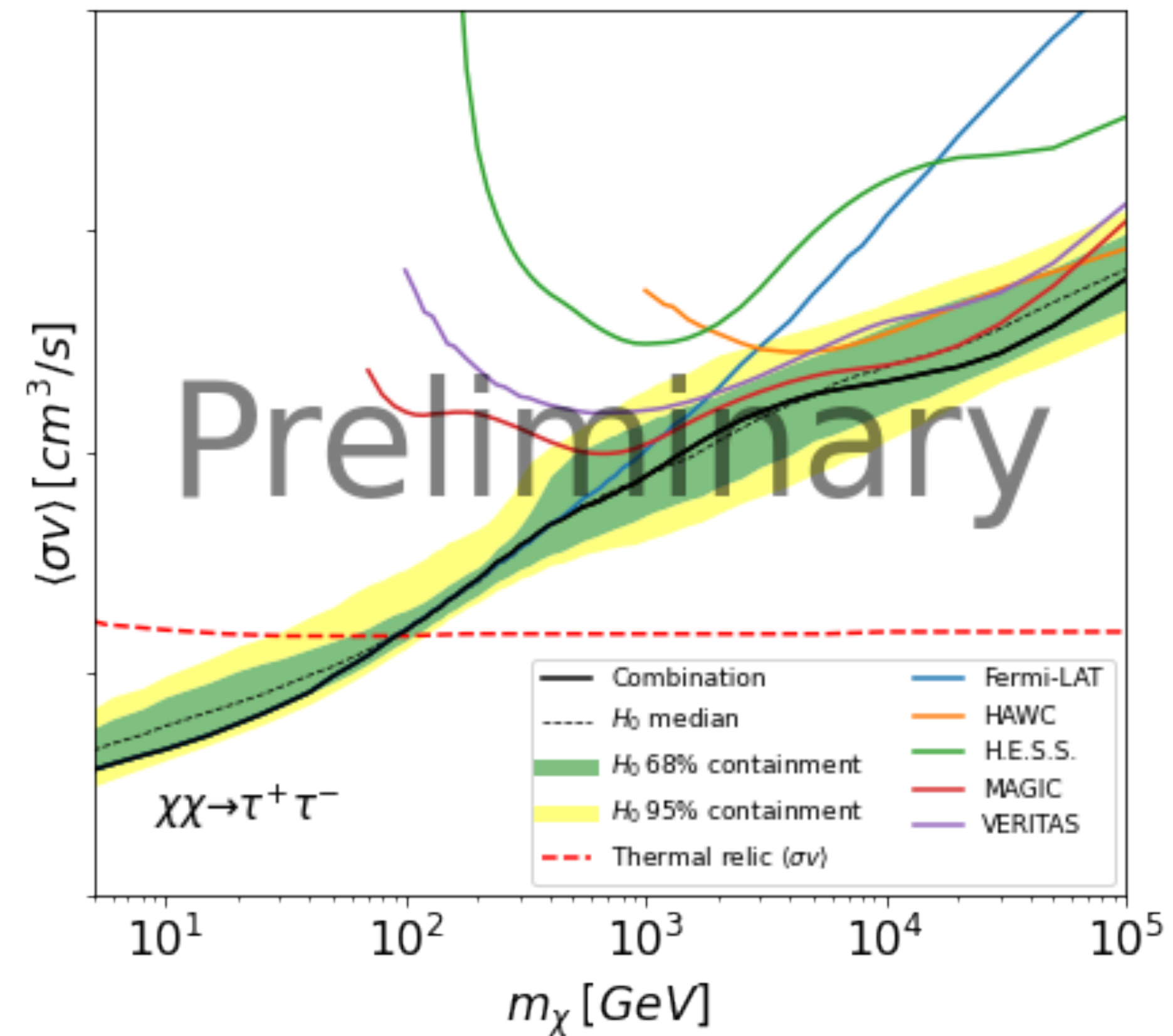
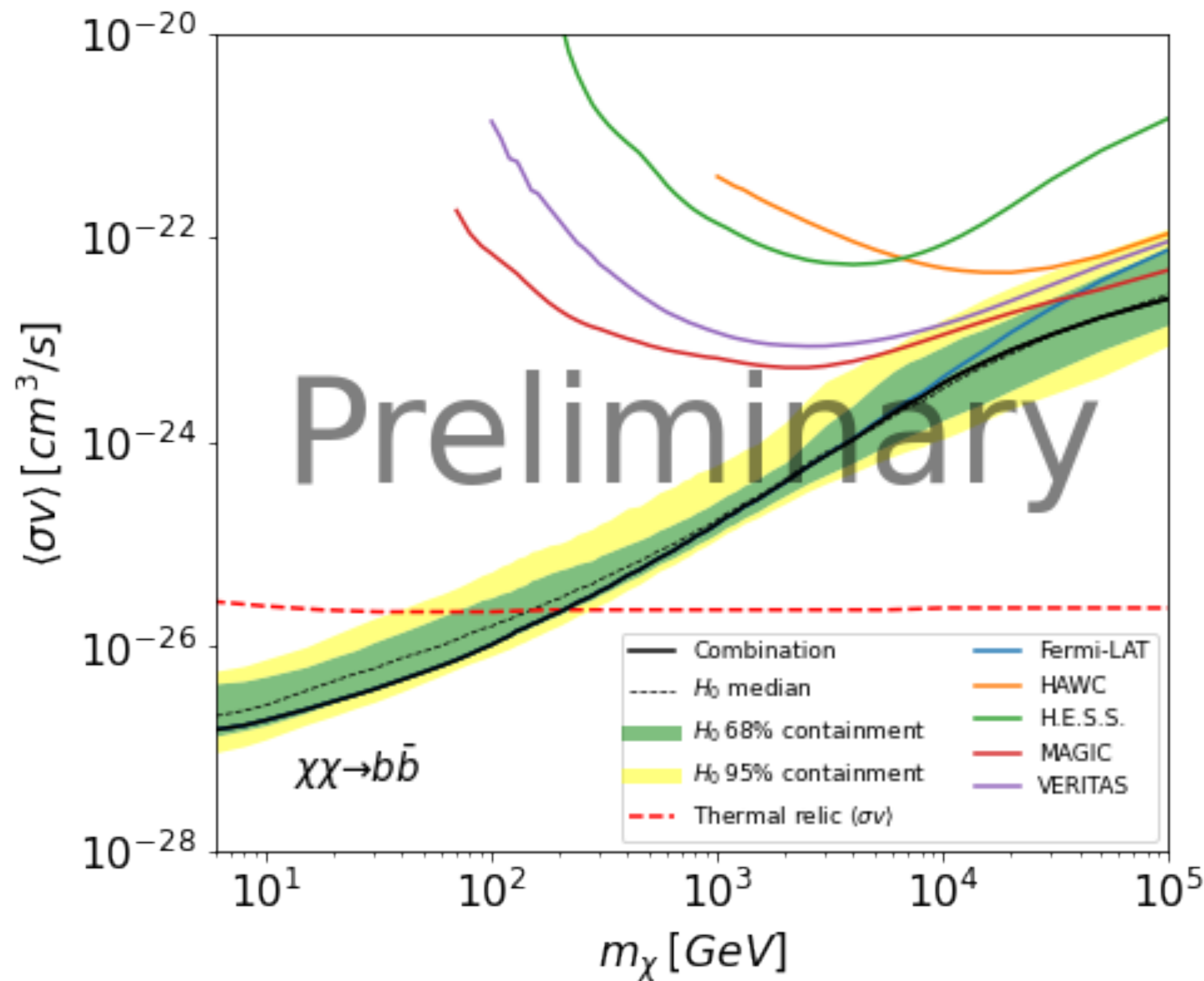
Mean of the derived $\langle\sigma v\rangle$ distribution

Statistical uncertainty bands

Standard deviation at 1 and 2σ

CONSTRAINTS ON DARK MATTER

Ref: PoS ICRC2021 (2021) 528, arXiv: 2108.13646



Combined upper limits are **2-3 times more constraining**

CONSTRAINTS ON DARK MATTER

NOTE THAT

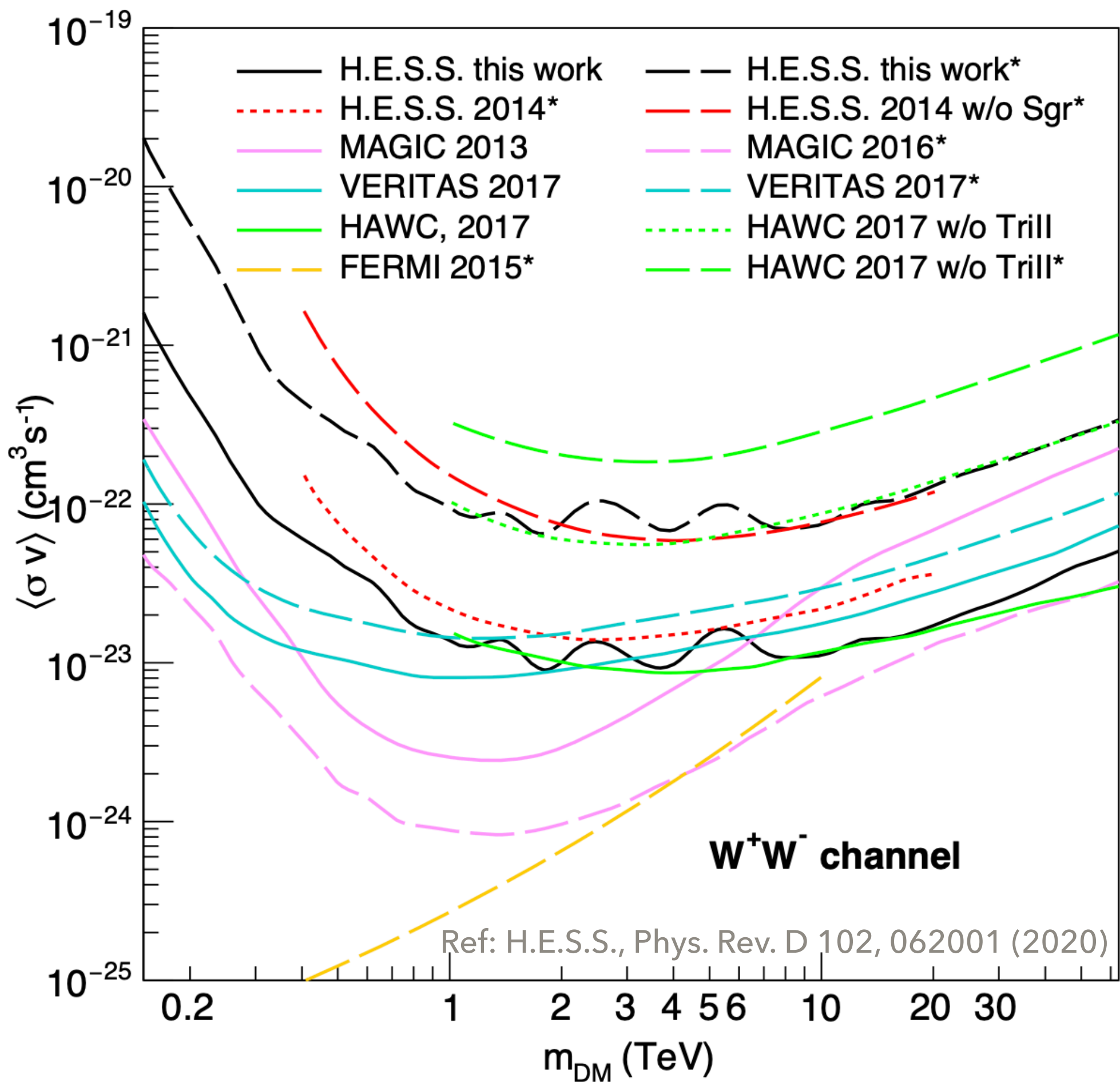


Upper limit profiles **depend on the choice** of the annihilation channel

Upper limits **driven by the objects with the highest J factors** that can be observed

Ultrafaint dSphs can be subject to **large systematic uncertainties** for the determination of their J-factors, e.g. Segue I

CONSTRAINTS ON DARK MATTER



Upper limits with the J nuisance increase up to a factor of 10.

- **H.E.S.S. - 5 ultrafaint dSphs**

High uncertainties compared to those of the classical dSphs
 Degradation of the upper limits

$\log_{10} J(0.125^\circ)$

Ret II - 19.2 ± 0.6

Tuc II - 18.4 ± 0.7

Tuc III - 18.8 ± 0.7

Tuc IV - 18.1 ± 0.7

Gru II - 18.1 ± 0.7

Ref: Bonnivard et al, 2015 ApJ 801 74

Ref: Walker et al., 2016 Astrophys. J.819, 53

Estimations from empirical law
 Ref: Fermi-LAT, Astrophys. J.834,110 (2017)

Typical values for classical dSphs

$\log_{10} J(0.125^\circ) \sim 17-18$

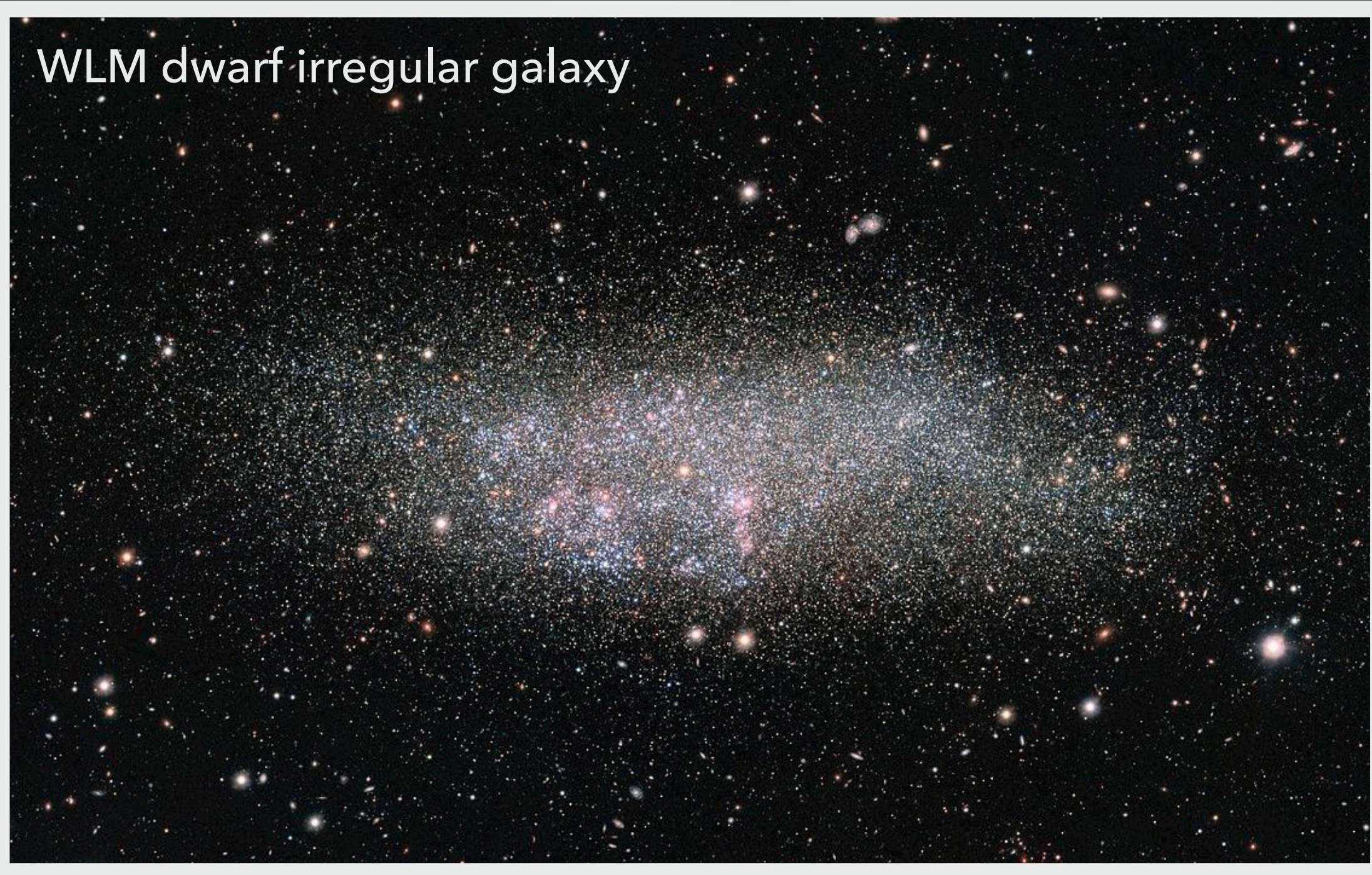
$\log_{10} \Delta J(0.125^\circ) \sim 0.1-0.3$

- Increase of the upper limits also in **HAWC (green)** and **VERITAS (blue)**

- The **increase of datasets** allows the derivation of **better upper limits** as in HESS (red) with/without sagittarius

Dwarf Irregular Galaxies

WLM dwarf irregular galaxy

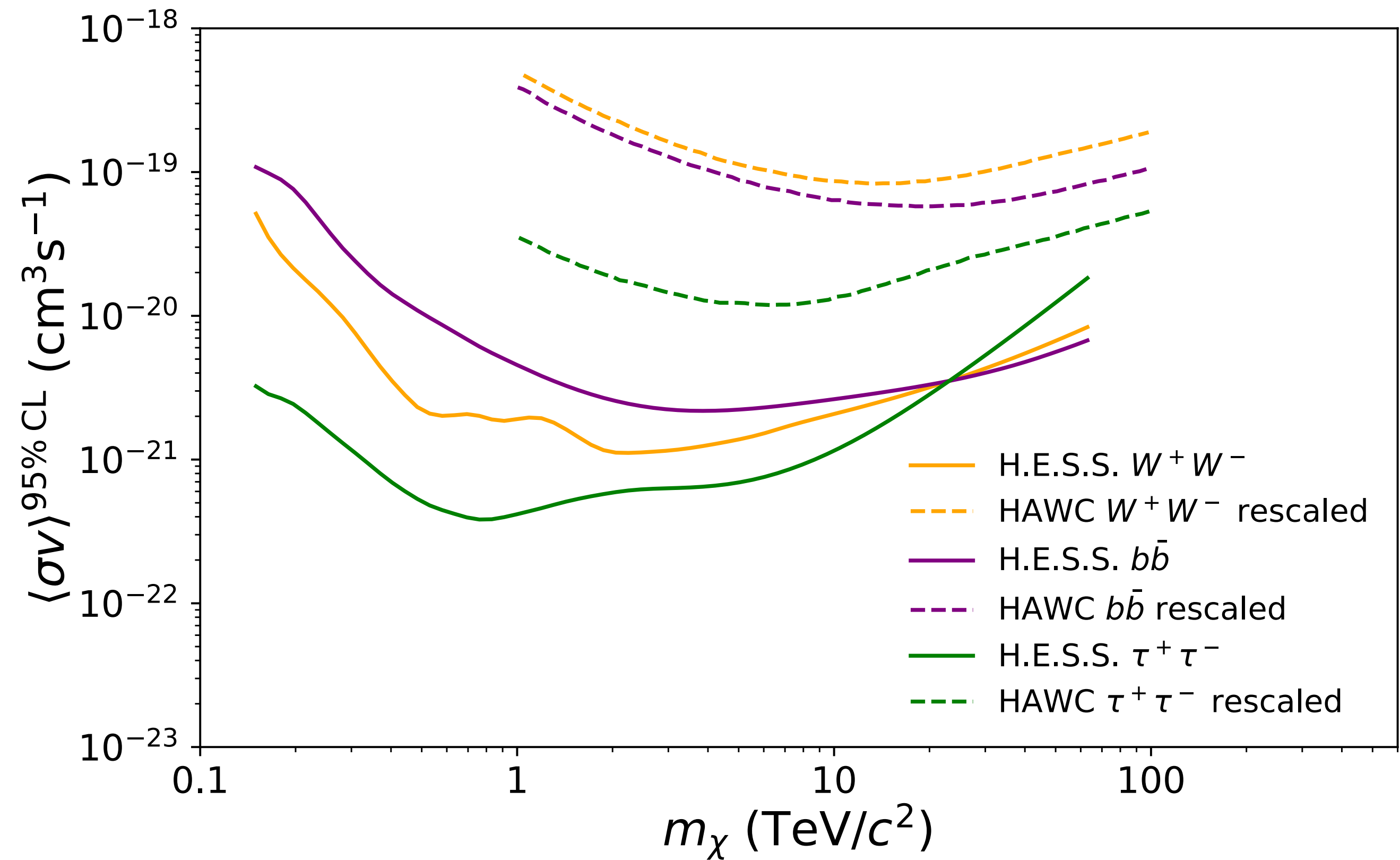
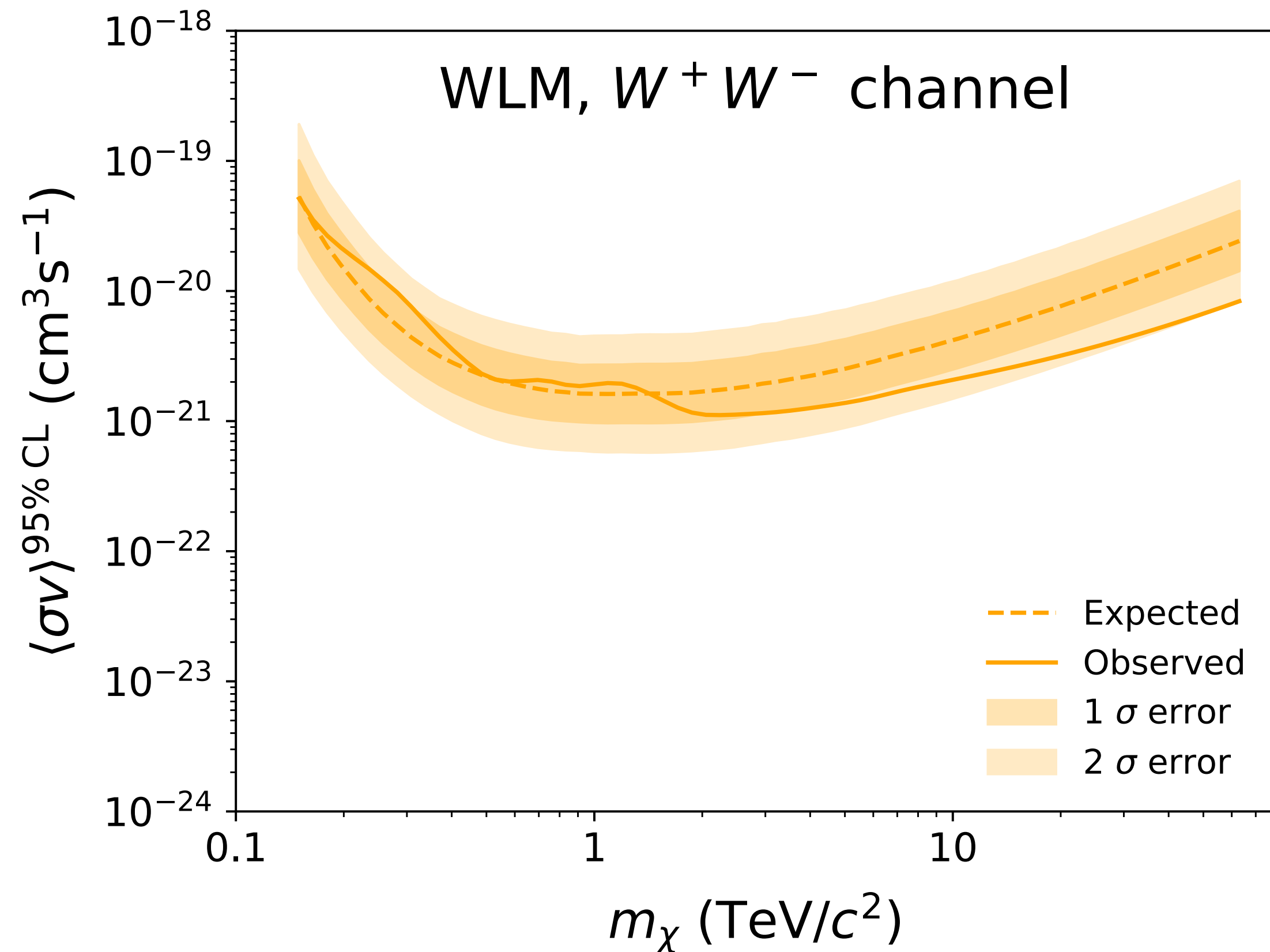


- Located between **~500 kpc and 1 Mpc**
- Dark matter **dominated**
- Contain **gas** (tracer)
- **Smooth** rotation curve
- **Smaller uncertainties** on their dark matter distribution and hence on the J factor

Case of WLM - $\log_{10} J(0.125^\circ) = 16.68 \pm 0.05$

Derivation from a **coreNFW** density profile

CONSTRAINTS ON DARK MATTER



Small uncertainties on the J factor

No visible degradation of the upper limits on the plot

H.E.S.S. limits up to **200x better** than those published by HAWC

DECAYING DARK MATTER

$$\frac{d\Phi(\tau_\chi, D)}{dE} = \frac{1}{4\pi} \frac{1}{\tau_\chi m_\chi} \sum_f \text{BR}_f \frac{dN_f}{dE} \times \int_{\Delta\Omega} \int_{\text{los}} \rho_{\text{DM}} ds d\Omega$$

Particle Physics
factor

D factor

Same procedure for limits derivation except that

J factor



D factor

$$\frac{\langle\sigma v\rangle}{2m_\chi^2}$$



$$\frac{1}{\tau_\chi m_\chi}$$

Upper limits

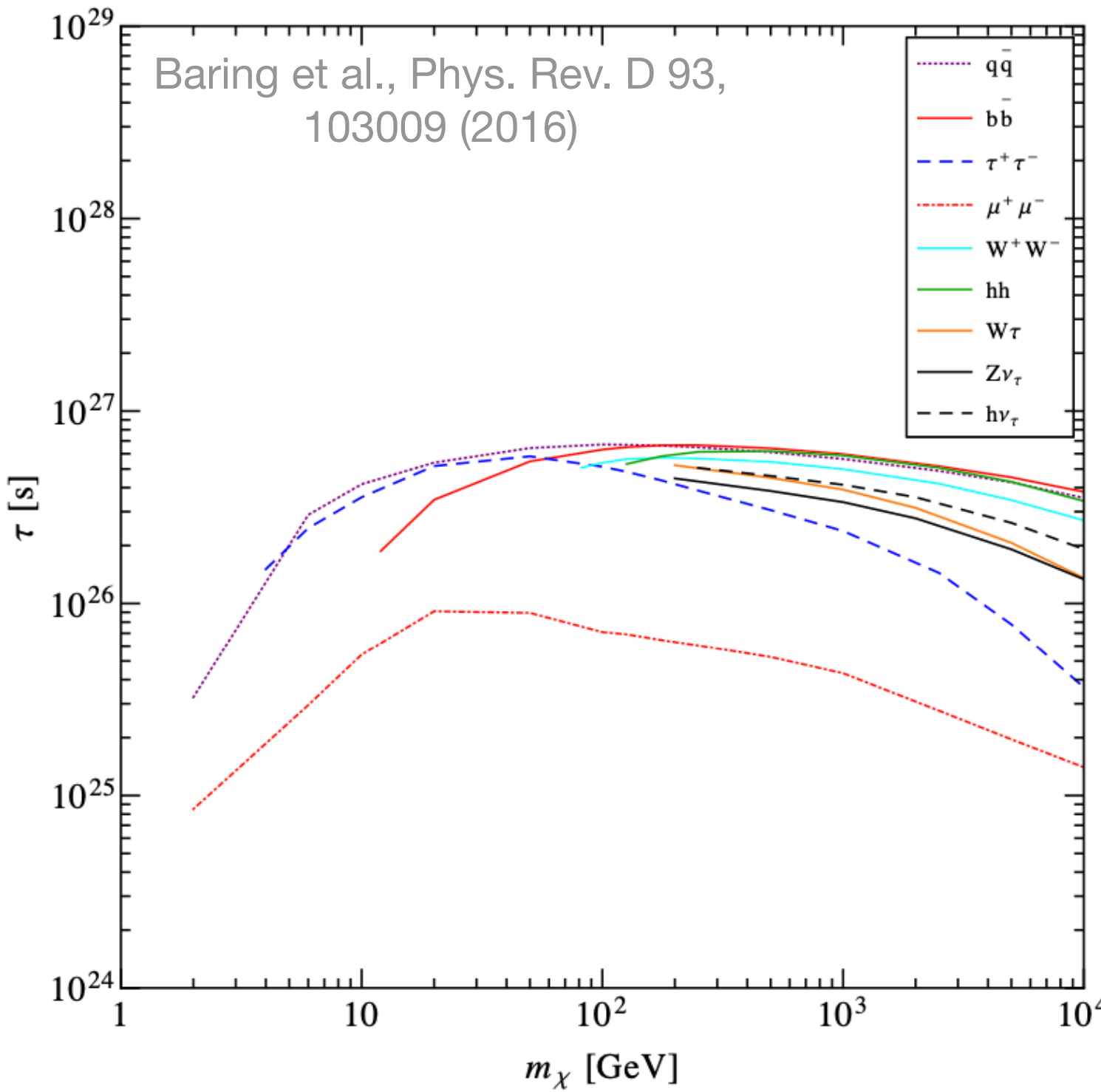


Lower limits

on the DM annihilation cross section

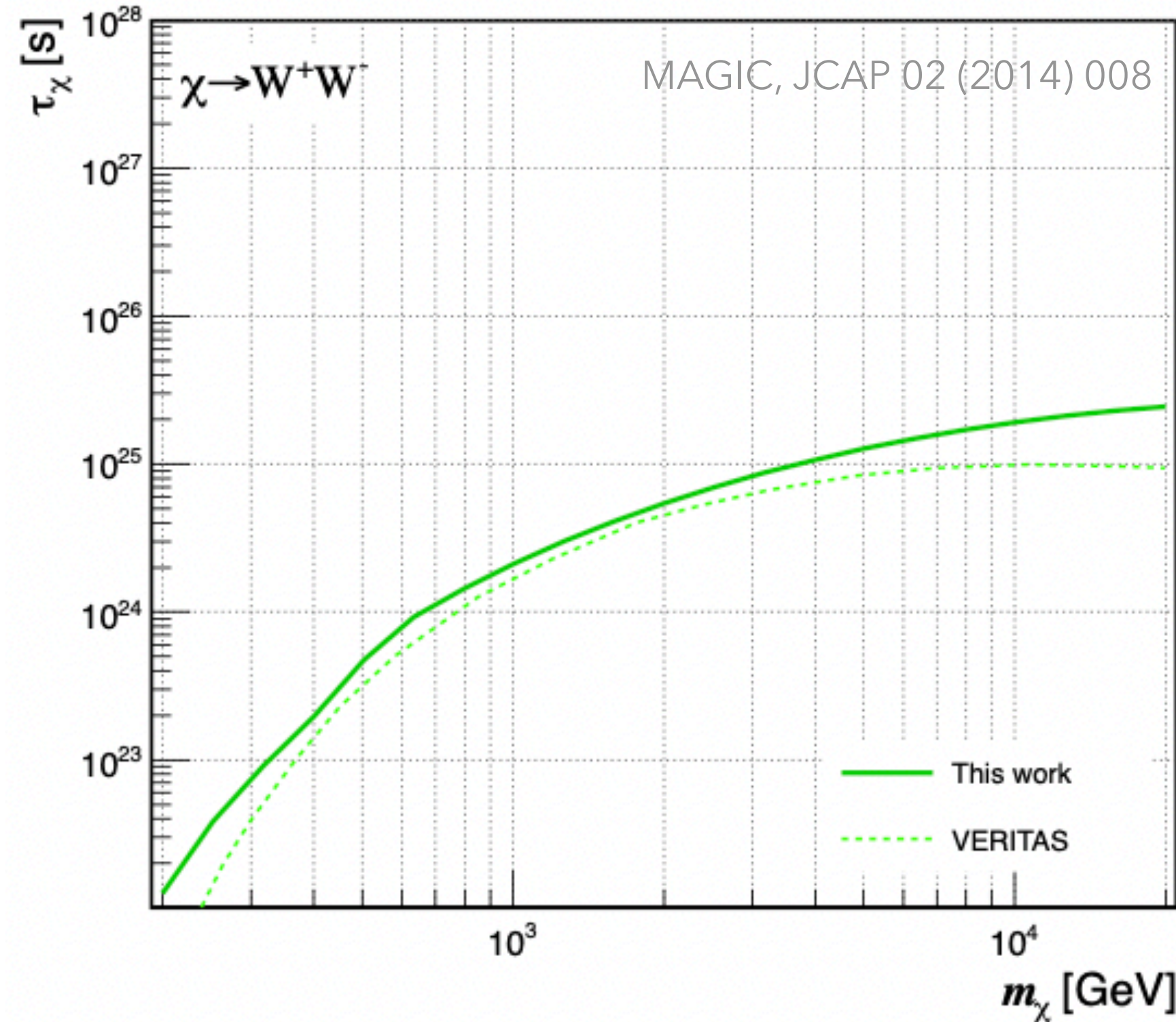
on the DM decaying lifetime

DECAYING DARK MATTER



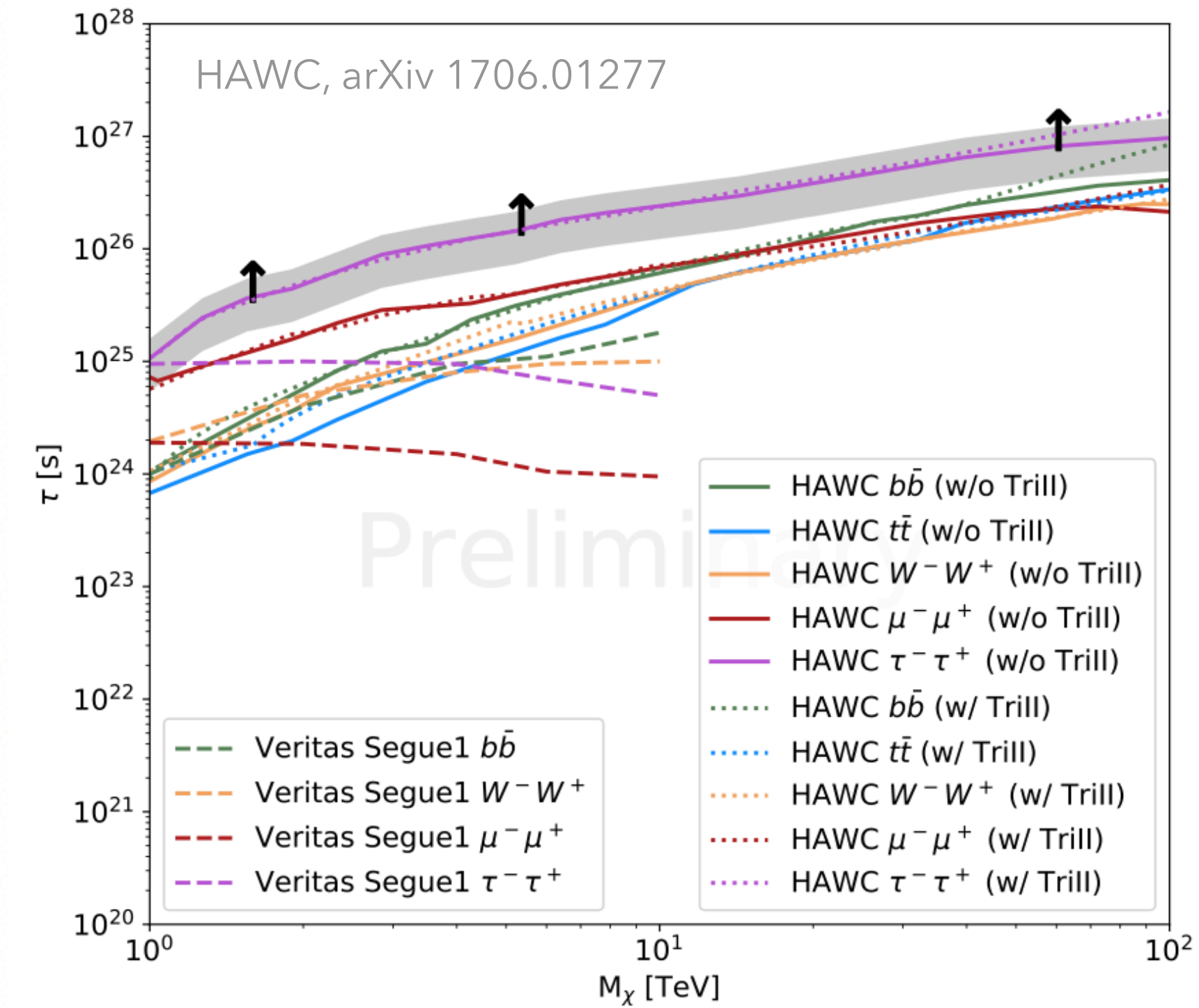
Fermi LAT

Combined lower limits with 15 dSphs
6 years of data



MAGIC (160h) and VERITAS (48h)

Segue I only



HAWC

Combined lower limits with 15 and 14 dSphs

Better lower limits with the combination of dSphs

TAKE AWAYS

- **No significant DM signal** observed by any of the experiments
- Use of the **likelihood profiling** to derive limits on the DM cross section/decay lifetime
- Collaborative effort to **combine individual results** between experiments
- **More competitive** upper limits over the **widest mass range ever** for the DM WIMPs
- Possible combination including **other messengers such as neutrinos** (already some contacts with IceCube and ANTARES/KM3NeT)
- **Future observations** of Sculptor (South hemisphere) and Draco (North hemisphere) with **CTA**
- **LHAASO experiment (2019)** in China could also provide **further competitive results**



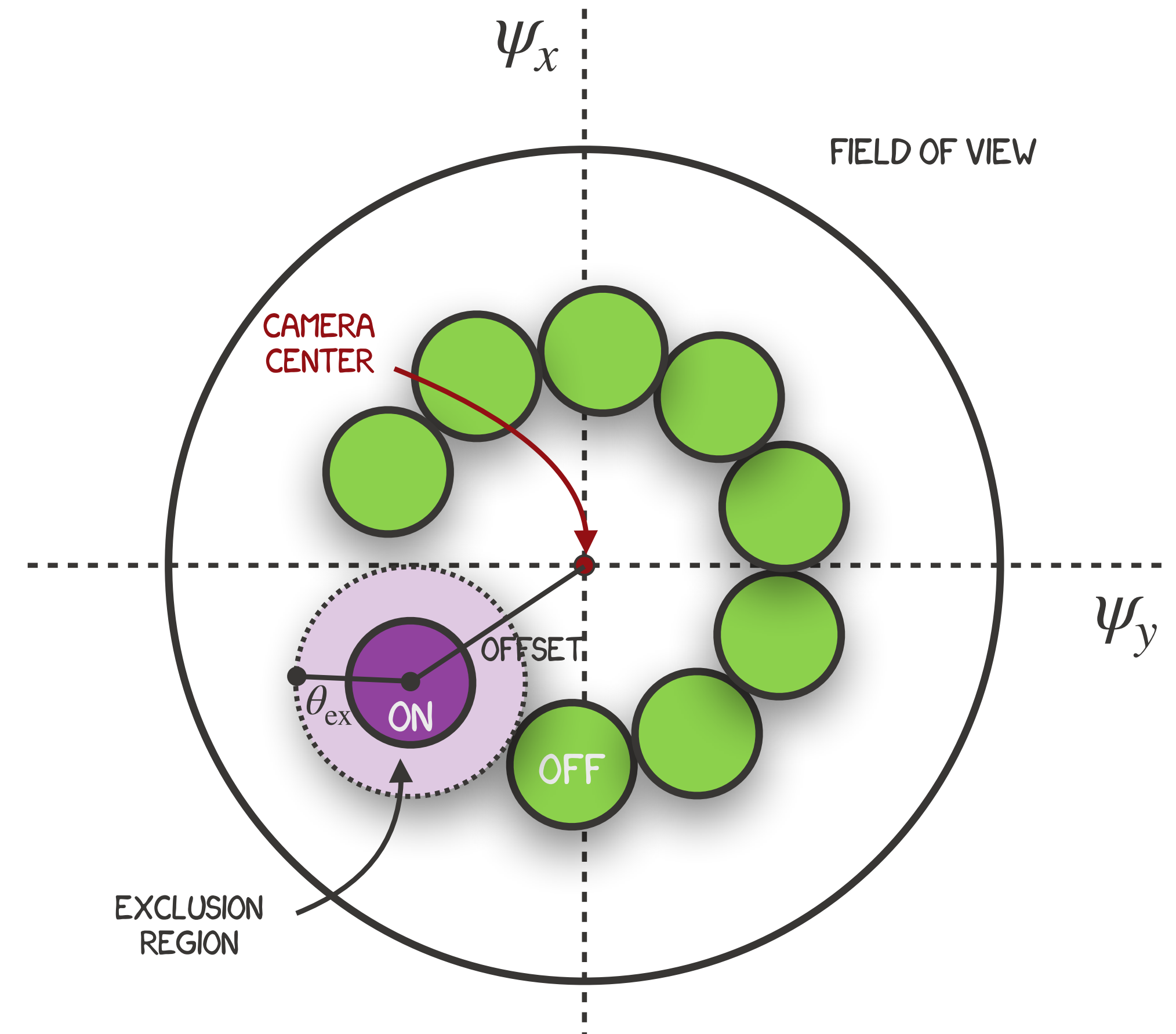
THANKS FOR YOUR ATTENTION!

BACKUP

DATA ANALYSIS IN H.E.S.S.

Multiple OFF technique

- **Pointing position slightly shifted** from the source position
- **Signal region** - ON region
- **Background region** - Many OFF regions distributed around the camera center



STATISTICAL ANALYSIS

Total likelihood

$$\mathcal{L}(\langle \sigma v \rangle, N_B, J) = \prod_{i=1} \mathcal{L}_{P_i}(\langle \sigma v \rangle, N_{B_i}, J | N_{\text{ON}_i}, N_{\text{OFF}_i}, \alpha) \mathcal{L}^J(J | \bar{J}, \sigma_J)$$

Poisson likelihood

Log-normal likelihood

Poisson likelihood for each energy bin

$$\mathcal{L}_i^P = \frac{(N_{S_i} + N_{B_i})^{N_{\text{ON}_i}}}{N_{\text{ON}_i}!} e^{-(N_{S_i} + N_{B_i})} \cdot \frac{(\alpha N_{B_i})^{N_{\text{OFF}_i}}}{N_{\text{OFF}_i}!} e^{-\alpha N_{B_i}}$$

ON REGION

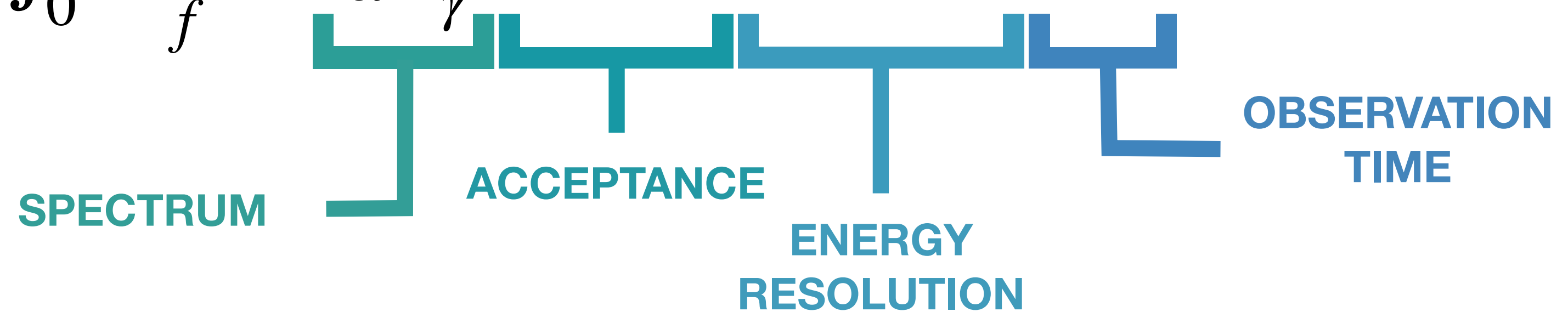
OFF REGION

Log-normal likelihood to model the uncertainties of the J factor

$$\mathcal{L}^J = \frac{1}{\ln(10)\sqrt{2\pi}\sigma_J J} \exp - \frac{(\log_{10} J - \log_{10} \bar{J})^2}{2\sigma_J^2}$$

STATISTICAL ANALYSIS

$$N_{S_i} = \frac{1}{2} \frac{\langle \sigma v \rangle}{4\pi m_\chi^2} J \int_{\Delta E_i} \int_0^\infty \sum_f B_f \frac{dN_\gamma^f}{dE_\gamma} A_{\text{eff}}(E_\gamma) R(E_\gamma, E'_\gamma) T_{\text{obs}} dE_\gamma dE'_\gamma$$



CONVOLUTION

SPECTRA
interpolated from Cirelli *et al.*, *JCAP* 1103, page 051.

X

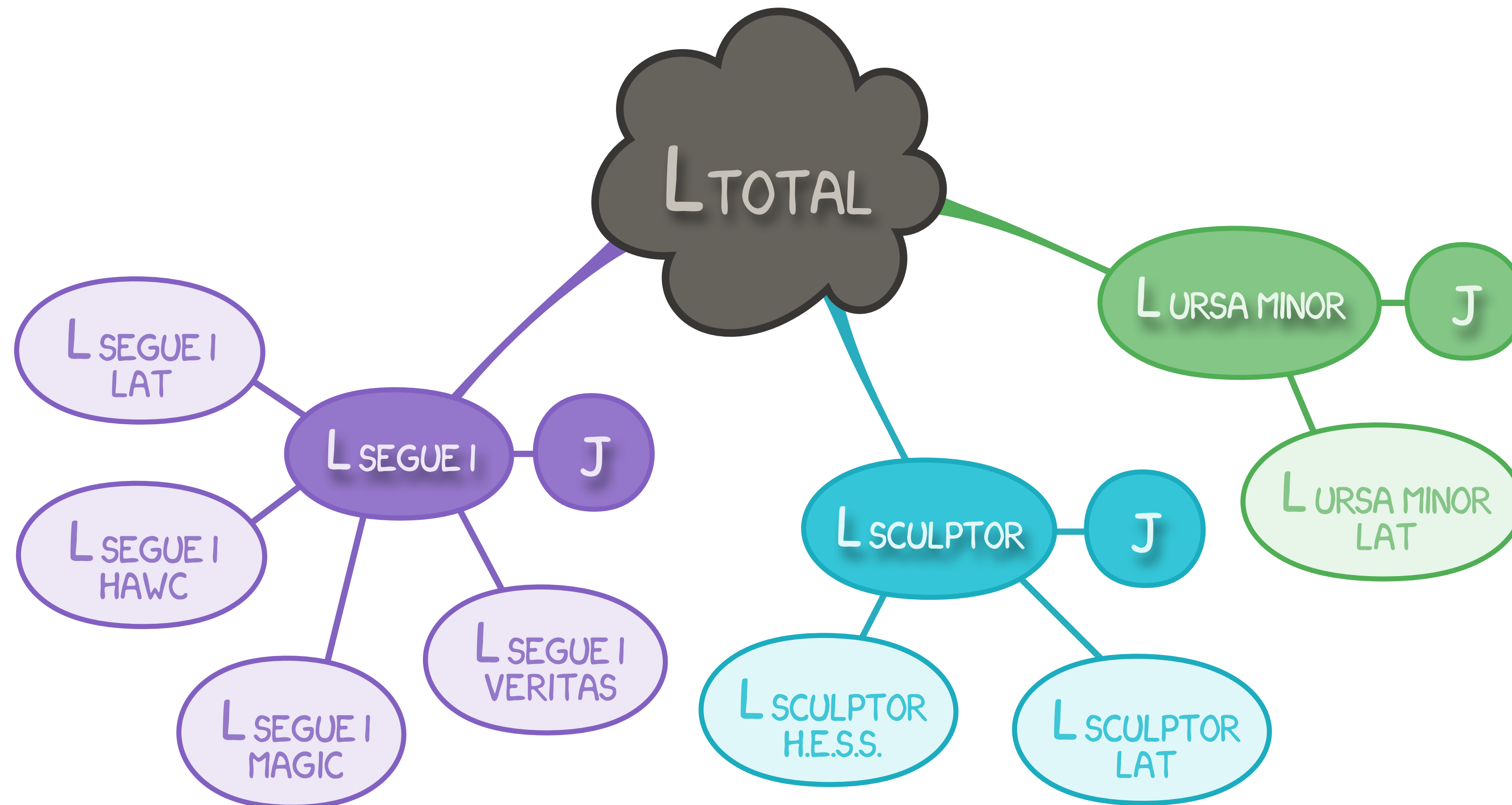
ACCEPTANCE
interpolated from the ParisAnalysis tables

X

ENERGY RESOLUTION
modeled by a Gaussian function

JOINT LIKELIHOOD ANALYSIS

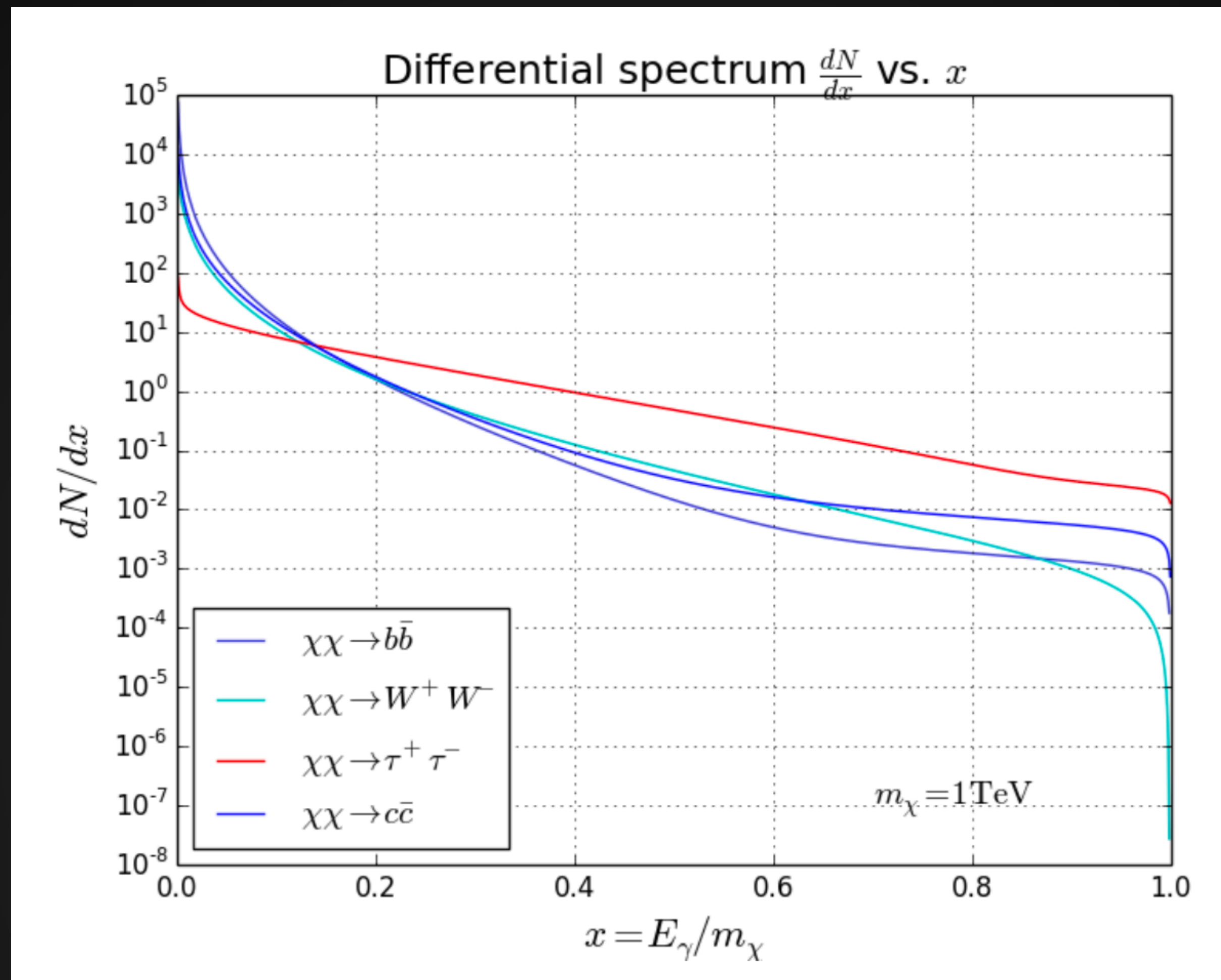
TOTAL LIKELIHOOD = PRODUCT OF INDIVIDUAL LIKELIHOODS



TARGETS

Name	Distance (kpc)	l, b ($^{\circ}$)	$\log_{10} J$ ($\mathcal{G}\mathcal{S}$ set) $\log_{10}(\text{GeV}^2\text{cm}^{-5}\text{sr})$	$\log_{10} J$ (\mathcal{B} set) $\log_{10}(\text{GeV}^2\text{cm}^{-5}\text{sr})$
Boötes I	66	358.08, 69.62	$18.24^{+0.40}_{-0.37}$	$18.85^{+1.10}_{-0.61}$
Canes Venatici I	218	74.31, 79.82	$17.44^{+0.37}_{-0.28}$	$17.63^{+0.50}_{-0.20}$
Canes Venatici II	160	113.58, 82.70	$17.65^{+0.45}_{-0.43}$	$18.67^{+1.54}_{-0.97}$
Carina	105	260.11, -22.22	$17.92^{+0.19}_{-0.11}$	$18.02^{+0.36}_{-0.15}$
Coma Berenices	44	241.89, 83.61	$19.02^{+0.37}_{-0.41}$	$20.13^{+1.56}_{-1.08}$
Draco	76	86.37, 34.72	$19.05^{+0.22}_{-0.21}$	$19.42^{+0.92}_{-0.47}$
Fornax	147	237.10, -65.65	$17.84^{+0.11}_{-0.06}$	$17.85^{+0.11}_{-0.08}$
Hercules	132	28.73, 36.87	$16.86^{+0.74}_{-0.68}$	$17.70^{+1.08}_{-0.73}$
Leo I	254	225.99, 49.11	$17.84^{+0.20}_{-0.16}$	$17.93^{+0.65}_{-0.25}$
Leo II	233	220.17, 67.23	$17.97^{+0.20}_{-0.18}$	$18.11^{+0.71}_{-0.25}$
Leo IV	154	265.44, 56.51	$16.32^{+1.06}_{-1.70}$	$16.36^{+1.44}_{-1.65}$
Leo V	178	261.86, 58.54	$16.37^{+0.94}_{-0.87}$	$16.30^{+1.33}_{-1.16}$
Leo T	417	214.85, 43.66	$17.11^{+0.44}_{-0.39}$	$17.67^{+1.01}_{-0.56}$
Sculptor	86	287.53, -83.16	$18.57^{+0.07}_{-0.05}$	$18.63^{+0.14}_{-0.08}$
Segue I	23	220.48, 50.43	$19.36^{+0.32}_{-0.35}$	$17.52^{+2.54}_{-2.65}$
Segue II	35	149.43, -38.14	$16.21^{+1.06}_{-0.98}$	$19.50^{+1.82}_{-1.48}$
Sextans	86	243.50, 42.27	$17.92^{+0.35}_{-0.29}$	$18.04^{+0.50}_{-0.28}$
Ursa Major I	97	159.43, 54.41	$17.87^{+0.56}_{-0.33}$	$18.84^{+0.97}_{-0.43}$
Ursa Major II	32	152.46, 37.44	$19.42^{+0.44}_{-0.42}$	$20.60^{+1.46}_{-0.95}$
Ursa Minor	76	104.97, 44.80	$18.95^{+0.26}_{-0.18}$	$19.08^{+0.21}_{-0.13}$

Twenty
Dwarf
Spheroidal
Galaxies



$$\tau^\pm \rightarrow h^\pm + \geq 1 \text{ neutral} + \nu_\tau$$

Some of the neutral particles produced are pions π^0 which, in turn, decay as $\pi^0 \rightarrow \gamma\gamma$. These processes are highly energetic and so are the emitted γ photons. By contrast with the τ , the quarks produced by dark matter annihilation hadronize combining with quarks and antiquarks spontaneously created from the vacuum. The new particles created lead to decay chains emitting lower energy γ . Furthermore, all curves have a quick decrease for $x \rightarrow 1$ as the energy of the particles produced cannot be greater than the energy of the initial particle.